Abrupt Fermi-Surface Change at the Quantum Critical Point in $YbRh_2Si_2$

Stefanie Hartmann, Sven Friedemann, Christoph Geibel, Cornelius Krellner, Niels Oeschler, Silke Paschen[1], Jörg Sichelschmidt, Steffen Wirth, Jan Wykhoff, and Frank Steglich

Introduction

Continuous phase transitions at zero temperature, referred to as quantum phase transitions or quantum critical points (QCP), and their consequences for the physical properties at finite temperatures have attracted considerable attention in recent years [1]. For so-called unconventional QCPs, a breakdown of the local Kondo energy scale and, correspondingly, a drastic change of the Fermi surface topology are expected along a crossover line T^*, concomitant to the localization of the *f* electrons on the magnetic side of the QCP [2]. The "Kondo breakdown" scenario seems to be realized for the heavy-fermion compound $YbRh_2Si_2$ whose low-temperature properties close to the QCP have extensively been studied within the last years. As shown in Fig. 1, the system orders antiferromagnetically at an extremely low temperature T_N = 70 mK. This order can be suppressed by the application of tiny magnetic fields $B_c \approx 60$ mT and $B_c \approx 700$ mT perpendicular and parallel to the tetragonal *c* axis, respectively [3]. For larger fields, a heavy Landau-Fermi-liquid (LFL) regime emerges below T_{LFL}. On the other hand, strong deviations from ordinary LFL behavior in large regions of the *T*-*B* phase diagram are observed in a number of properties. For instance, the Sommerfeld coefficient of the electronic specific heat shows a divergent behavior at the critical field, while the resistivity is linear in temperature [4]. Clear non-Fermi-liquid (NFL) behavior was recently inferred from far-infrared optical conductivity experiments down to T = 0.4 K [5]. Furthermore, the temperature dependence of the Grüneisen parameter disagrees with theoretical predictions for a conventional QCP [6].

A new crossover energy scale, $T^*(B)$, was detected in a number of transport and thermodynamic properties (cf. Fig. 1) in agreement with the predictions of the above-mentioned "Kondo breakdown" scenario. In particular, Hall-effect measurements indicated an abrupt jump of the Fermi surface at the QCP in $YbRh_2Si_2$ [7]. Subsequent magnetization and magnetostriction measurements confirmed $T^*(B)$ to be an additional energy scale disparate from both $T_N(B)$ and $T_{LFL}(B)$, cf. Fig. 1 [8]. The ESR results also show a crossover behavior, as inferred from the evolution of the g factor and the ESR linewidth [9]. While in the paramagnetic LFL regime heavy quasi-particles with strong *f* character form a large Fermi surface, the 4*f* states are assumed to fully localize on the low-field side of the QCP resulting in a small Fermi surface.

Information on the evolution of the Fermi surface in $YbRh_2Si_2$ may be drawn from de Haas - van Alphen experiments [10] and angle-resolved photoemission spectroscopy [11]. However, the former experiments were restricted to high fields, $B >> B_c$, and the latter to high temperatures, $T >> T_N$. This motivated further studies on the Hall effect and the thermopower of new, high-quality $YbRh_2Si_2$ samples as presented in the following. For $YbRh_2Si_2$, the normal contribution to the Hall coefficient was shown to be dominant at low temperatures. Hence, it provides a direct measure of the charge-carrier density [12]. The diffusion part of the thermopower in heavy-fermion systems is proportional to the energy derivative of the density of states (DOS) of the heavy quasiparticles at the Fermi energy.

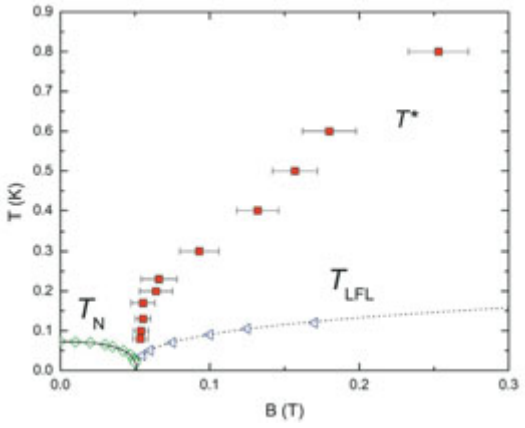

Fig. 1: T–B phase diagram of $YbRh_2Si_2$, according to [8]. The magnetic field B is applied perpendicular to the c axis. T_N and T_{LFL} are deduced from resistivity data, T^* from magnetostriction.

Hall effect measurements

Detailed Hall effect measurements have been repeated in a new low-temperature setup with improved resolution on new single crystals. In particular, two magnetic fields were generated by a vector magnet, simultaneously probing the Hall voltage and tuning the system through the quantum critical regime. The current was injected parallel to the tetragonal basal plane, and the magnetic field B_1 inducing the Hall voltage V_{xy} was applied along the crystallographic c axis. The Hall resistivity was obtained from the asymmetric component of the field-inversed Hall voltage. A longitudinal field B_2 is applied parallel to the current to tune the underlying ground state while generating essentially no Hall response. The field B_1 should only probe the linear Hall response and thus has to be small compared with the characteristic tuning fields. Taking advantage of the anisotropy allows us to apply fields along the magnetically hard c axis which are about a factor of 10 higher than within the basal plane.

The results of the isothermal crossed-field measurements at low temperatures are presented in Fig. 2. At all temperatures, a pronounced crossover from a zero-field value to the substantially reduced high-field value is observed. As the temperature is raised, the inflection point of the crossover structure moves toward larger fields. At the same time, the crossover broadens. Following the procedure described in [8] the data were fitted by an empirical formula taking into account an appropriate background contribution. This function simulates a step-like shape of the field-dependent Hall coefficient. It includes the absolute values at $B = 0$, R_H^0, and at higher fields, R_H^∞, the sharpness of the crossover as well as the field of the inflection point, B_0. The position of the inflection point corresponds to the $T^*(B)$ line deduced from magnetic and transport properties. The jump height (R_H^0-R_H^∞) decreases for decreasing T, yet remains finite for $T \rightarrow 0$. Furthermore, the width of the crossover is proportional to temperature. Consequently, in the zero-temperature extrapolation, the Hall coefficient exhibits a discontinuous jump at the critical field.

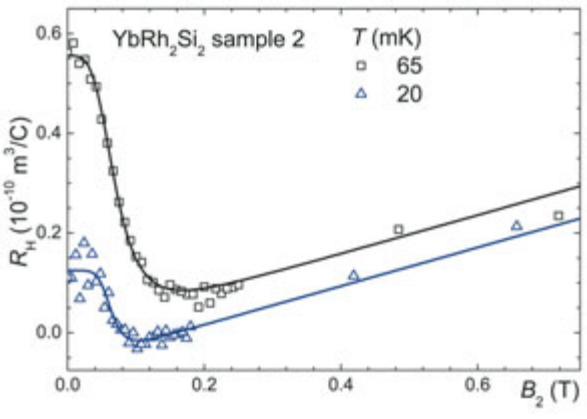

Fig. 2: Hall coefficient R_H of $YbRh_2Si_2$ vs. B_1 for temperatures 20 mK and 65 mK. Solid lines represent best fits to the data with the empirical crossover formula $R_H = R_H^\infty + mB_2 - (R_H^\infty + mB_2 - R_H^0)/(1-(B_2/B_0)^p)$ which allows to extract the position of the crossover B_0 as well as its width.

These results confirm the previous interpretation of the Hall effect data in [8]. However, due to an improved resolution and extended temperature and field ranges, the zero-field extrapolation could be performed with higher accuracy. The Hall effect as well as magnetoresistance measurements provide strong support to the local "Kondo breakdown" scenario being realized in $YbRh_2Si_2$.

Thermopower measurements

By means of a new low-T thermal transport set-up that utilizes a "one heater-two thermometers" technique the available temperature range has been extended down to 30 mK [13]. Excellent agreement of the new thermopower $S(T)$ measurements between 30 mK and 6 K compared to previous results is obtained in the overlap range 1.8 - 6 K.
The thermopower of $YbRh_2Si_2$ exhibits strongly enhanced, negative values below room temperature. A broad minimum around 80 K (not shown) is attributed to a combination of Kondo scattering and crystal electric field effects [14,15]. The negative sign is typically observed in Yb-based heavy-fermion system with a narrow Kondo resonance peak slightly below the Fermi energy. In Fig. 3 the thermopower of $YbRh_2Si_2$ is plotted as $-S(T)/T$ vs. log T for selected fields. In zero fields, $|S|/T$ exhibits a logarithmic increase over one decade in temperature between 1 K and 0.1 K [16]. It passes over a maximum around $T_{max} \approx 0.1$ K with strongly enhanced values of 15 $\mu V/K^2$, before it decreases and changes sign at $T_0 \approx 30$ mK, cf. inset of figure 3. In contrast to specific heat, $c_p(T)$, and resistivity, $\rho(T)$, results [4], no signature of the antiferromagnetic phase transition at $T_N = 70$ mK

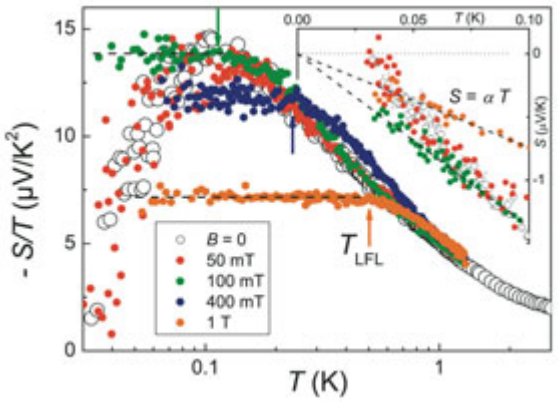

Fig. 3: Negative thermopower divided by T, -S(T)/T, of $YbRh_2Si_2$ in different magnetic fields on a logarithmic T scale. The dashed lines indicate a constant -S/T for $B>B_c$ characteristic of LFL behavior. The NFL-LFL crossover temperatures, T_{LFL}, are marked by arrows. Inset: Low-temperature part of S(T) on a linear T scale. A sign change from negative to positive appears near T_0 = 30 mK for B = 0 T and 50 mT. The dashed lines represent fits to the data according to $S = \alpha T$.

is observed in the thermopower data. For all fields below the critical field, an almost identical behavior is found. At higher fields $B > B_c$, the low-T behavior changes drastically, cf. in Fig. 3 for B = 0.1, 0.4 and 1 T. Here, the thermopower remains negative even in the zero-temperature limit and is proportional to T below T_{LFL}, which corresponds to a saturation of $S(T)/T=\alpha$.

The observed behavior of $S(T)$ with large, constant values α is characteristic for a heavy LFL state, in agreement with previous $c_p(T)/T$ and $\rho(T)$ results. The range with constant $S(T)/T$ is enlarged upon increasing field and concomitantly, the absolute value of α decreases. The NFL-LFL crossover temperature T_{LFL} fully coincides with the one derived from resistivity measurements on the same sample with the same contact geometry [16]. The thermopower results on $YbRh_2Si_2$ are thus in good agreement with the established phase diagram [4,8].

The logarithmic increase of $|S|/T$ in zero field signals non-Fermi liquid behavior. This agrees with specific heat results that showed a similar behavior in a comparable temperature range [3,17]. In fact, theoretical calculations within the two-dimensional spin-density wave scenario yielded a logarithmic temperature dependence for both quantities in the non-Fermi liquid regime [18]. Almost the same temperature dependence is expected for the "Kondo breakdown" scenario [16].

The evolution of the thermopower with field is not continuous. Rather, a distinct change in the low-T behavior is observed when crossing the critical field B_c. To illustrate this, Fig. 4 shows a blow-up of the T-B phase diagram around the critical point. The temperatures of the sign change in $S(T)$, T_0, and of the maximum in $S(T)/T$, T_{max}, are plotted together with the antiferromagnetic ordering temperature, T_N, determined from $\rho(T)$ measurements, and the crossover temperatures T_{LFL} and T^*. T_N is continuously suppressed to zero at B_c = 64 mT, beyond which field the LFL phase emerges. By contrast, T_0 and T_{max} are field independent below B_c within experimental resolution, but vanish abruptly upon crossing the T^* line. In view of the fact that neither T_0 nor T_{max} do follow the field dependence of T_N, they can, consequently, not be related to the magnetic ordering in $YbRh_2Si_2$. In the zero-temperature limit, $S(T)/T$ exhibits a negative sign on the paramagnetic side of the QCP, whereas it is positive on the magnetic side. Since the thermopower reflects the energy dependence of the heavy quasi-particle DOS at the Fermi energy, the sudden sign change of $S(T\rightarrow 0)$ upon increasing the magnetic field beyond B_c reflects a dramatic change of the topology of the renormalized Fermi surface when crossing the field-induced QCP. These observations support the above conclusion from Hall-effect results. The

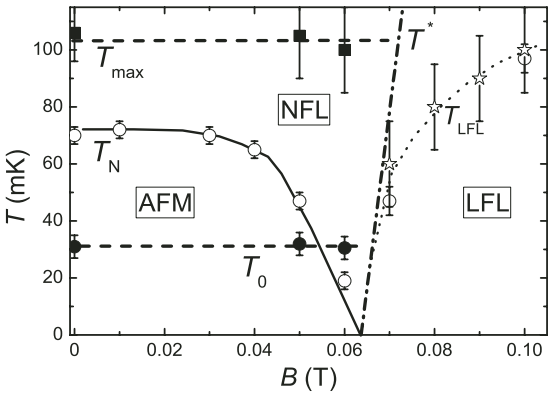

Fig. 4: Detailed phase diagram of $YbRh_2Si_2$ around the QCP. The field dependence of the antiferromagnetic ordering temperature T_N is compared to the temperatures of the sign change T_0 and of the maximum T_{max} in -S(T)/T. T_N was derived from $\rho(T)$ results on the same sample. The NFL-LFL crossover temperature T_{LFL} was obtained either from $\rho(T)$ (onset of $\Delta\rho \propto T^2$, open circles) or from S(T) measurements (onset of $S \propto T$, stars). $T_N(B)$ and $T_{LFL}(B)$ extrapolate to a critical field $B_c \approx 64$mT. The dotted lines are guides to the eye. The crossover line $T^*(B)$ was taken from [8] and scaled to B_c of the particular sample.

latter reveal a jump in the Hall coefficient $R_H(T\rightarrow 0)$ in the zero-temperature limit and, thus, a jump in the Fermi volume at the QCP with a localization of the 4*f* states on the low-field side [8]. The positive sign of *S(T)* of $YbRh_2Si_2$ in the "localized" regime for $B < B_c$ is in agreement with the findings for the non-magnetic counterpart $LuRh_2Si_2$ [14]. The field-induced sign change of $S(T\rightarrow 0)$ at B_c, as inferred from Figs. 2 and 3, provides convincing evidence of a Fermi surface reconstruction, consistent with a break-down of the effective Kondo scale at the antiferromagnetic QCP in $YbRh_2Si_2$.

Conclusions

A new energy scale, $T^*(B)$, which adds to the well established $T_N(B)$ and $T_{LFL}(B)$ scales was detected in $YbRh_2Si_2$ by means of thermodynamic and transport properties. All three scales merge at B_c, the critical field of the antiferromagnetic ordering. High-resolution Halleffect experiments show a step-like crossover at $T^*(B)$, which becomes a discontinuous jump as $T\rightarrow 0$. This implies a drastic change of the effective charge-carrier density at the QCP.

The low-temperature thermopower reveals a sudden sign change at the critical field B_c in the zero-temperature limit, which supports the reconstruction of the Fermi surface at the QCP in $YbRh_2Si_2$.

The transport and thermotransport results presented here reveal strong evidence for the break-down of the local Kondo scale at the QCP. At the paramagnetic side, the Fermi surface contains composite quasi-particles, whose *f* contribution seems to localize on the magnetic ground-state side of the QCP.

[1] Technical University of Vienna, Vienna, Austria

References

[1] *P. Gegenwart, Q. Si, F. Steglich,* Nature Physics **4,** (2008) 186.

[2] *Q. Si et al.,* Nature **413** (2001) 804.

[3] *O. Trovarelli, C. Geibel, S. Mederle, C. Langhammer, F.M. Grosche, P. Gegenwart, M. Lang, G. Sparn, and F. Steglich,* Phys. Rev. Lett. **85**, (2000) 626.

[4] *J. Custers, P. Gegenwart, H. Wilhelm, K. Neumaier, Y. Tokiwa, O. Trovarelli, C. Geibel, F. Steglich, C. Pépin, and P. Coleman,* Nature **424** (2003) 524.

[5] *S. Kimura, J. Sichelschmidt, J. Ferstl, C. Krellner, C. Geibel, and F. Steglich,* Phys. Rev. B **74** (2006) 132408.

[6] *R. Küchler, N. Oeschler, P. Gegenwart, T. Cichorek, K. Neumaier, O. Tegus, C. Geibel, J.A. Mydosh, F. Steglich, L. Zhu, and Q. Si,* Phys. Rev. Lett. **91** (2003) 066405.

[7] *S. Paschen, T. Lühmann, S. Wirth, P. Gegenwart, O. Trovarelli, C. Geibel, F. Steglich, P. Coleman, and Q. Si,* Nature **432** (2004) 881.

[8] *P. Gegenwart, T. Westerkamp, C. Krellner, Y. Tokiwa, S. Paschen, C. Geibel, F. Steglich, E. Abrahams, and Q. Si,* Science **315** (2007) 969.

[9] *U. Schaufuss, V. Kataev, A. A. Zvyagin, B. Büchner, J. Sichelschmidt, J. Wykhoff, C. Krellner, C. Geibel and F. Steglich,* Phys. Rev. Lett. **102** (2009) 076405.

[10] *P.M.C. Rourke et al.,* Phys. Rev. Lett. **101** (2008) 237205.

[11] *S. Danzenbächer et al.,* Phys. Rev. B **75** (2007) 045109.

[12] *S. Friedemann, N. Oeschler, C. Krellner, C. Geibel, S. Wirth, F. Steglich, S. Paschen, S. Maquilon, Z. Fisk,* Physica B **403** (2008) 1251.

[13] *S. Hartmann, N. Oeschler, C. Krellner, C. Geibel, and F. Steglich,* J. Phys.: Conference series, **150** (2009) 042049.

[14] *U. Köhler, N. Oeschler, F. Steglich, S. Maquilon, and Z. Fisk,* Phys. Rev. B **77** (2008) 104412.

[15] *S. Hartmann, U. Köhler, N. Oeschler, S. Paschen, C. Krellner, C. Geibel, and F. Steglich,* Physica B **378-380** (2006) 70.

[16] *S. Hartmann, N. Oeschler, C. Krellner, C. Geibel, S. Paschen, F. Steglich,* to be published (2009).

[17] *N. Oeschler, S. Hartmann, A.P. Pikul, C. Krellner, C. Geibel, and F. Steglich,* Physica B **403** (2008) 1254.

[18] *I. Paul and G. Kotliar,* Phys. Rev. B **64** (2001) 184414.